

Published in final edited form as:

FEBS Lett. 2013 June 5; 587(11): 1638–1643. doi:10.1016/j.febslet.2013.03.038.

Levels of Supramolecular Chirality of Polyglutamine Aggregates Revealed by Vibrational Circular Dichroism

Dmitry Kourouski^a, Karunakar Kar^{b,c}, Ronald Wetzel^{b,c}, Rina K. Dukor^d, Igor K. Lednev^{a,*}, and Laurence A. Nafie^{d,e,*}

^aUniversity at Albany, State University of New York, Albany, NY, 12222, USA

^bDepartment of Structural Biology, University of Pittsburgh School of Medicine, Pittsburgh, Pennsylvania 15260, USA

^cPittsburgh Institute for Neurodegenerative Diseases, University of Pittsburgh School of Medicine, Pittsburgh, Pennsylvania 15260, USA

^dBioTools, Inc., 17546 BeeLi60ne Hwy, Jupiter, Florida, 33458, USA

^eDepartment of Chemistry, Syracuse University, Syracuse, New York, 13244, USA

Abstract

Polyglutamine (PolyQ) aggregates are a hallmark of several severe neurodegenerative diseases, expanded CAG-repeat diseases in which inheritance of an expanded polyQ sequence above a pathological threshold is associated with a high risk of disease. Application of vibrational circular dichroism (VCD) reveals that these PolyQ fibril aggregates exhibit a chiral supramolecular organization that is distinct from the supramolecular organization of previously observed amyloid fibrils. PolyQ fibrils grown from monomers with Q repeats 35 and above (Q₃₅) exhibit approximately 10-fold enhancement of the *same* VCD spectrum compared to the already enhanced VCD of fibrils formed from Q repeats 30 and below (Q₃₀).

Keywords

Polyglutamine; PolyQ; fibril aggregates; chirality; vibrational circular dichroism; VCD; deep ultraviolet resonance Raman spectroscopy; DUVRR; hydrogen-deuterium exchange; CAG-repeat; neurodegenerative diseases

© 2013 Federation of European Biochemical Societies. Published by Elsevier B.V. All rights reserved.

*Corresponding author: Laurence A. Nafie, PhD., Addresses: Department of Chemistry, Syracuse University, Syracuse, New York, 13244, USA and BioTools, Inc., 17546 Beeline Hwy, Jupiter, Florida, 33458, USA., Phone: +1-561-625-0133, Fax: +1-516-625-0717, lanafie@syr.edu.

CONFLICT OF INTEREST

The authors declare no financial or commercial conflict of interest.

Supporting Information

Supporting Figures S1, S2 and S3 are available.

Publisher's Disclaimer: This is a PDF file of an unedited manuscript that has been accepted for publication. As a service to our customers we are providing this early version of the manuscript. The manuscript will undergo copyediting, typesetting, and review of the resulting proof before it is published in its final citable form. Please note that during the production process errors may be discovered which could affect the content, and all legal disclaimers that apply to the journal pertain.

INTRODUCTION

Supramolecular chirality is a distinct property of all macromolecules found in living organisms. Beyond individual small molecules, macromolecular structures can adopt a higher level of chirality, such as the α -helix of proteins and the B-helix of DNA, in which the chiral sense of helical structure has its origins in the chirality of its individual amino acid or sugar constituents. The hierarchy of chiral structure and organization can be traced to even higher levels of supramolecular chirality leading, in most cases, to a distinct handedness in the resulting biological structure, such as protein-RNA complexes, DNA-histone assemblies, and eventually to even higher levels of biological organization associated with physical morphology. Here we demonstrate that vibrational circular dichroism (VCD) reveals two levels of supramolecular chiral organization in polyglutamine (PolyQ) fibrils having their origins beyond the local secondary structure of the constituent polypeptide molecules. This structural distinction has not been detected by any previous imaging or spectroscopic analyses.

Amyloid fibrils are β -sheet rich protein aggregates that are often detected in organs and tissues of patients diagnosed with different neurodegenerative diseases and other maladies associated with protein misfolding.^{1,2} Application of electron microscopy (EM) and atomic force microscopy (AFM) has revealed a high morphological heterogeneity of amyloids, a phenomenon known as fibril polymorphism.³⁻⁶ These and other microscopic tools, however, may provide only limited information about fibril chirality.⁷ This limit lies at the level of imaged fibril handedness and none of these techniques appears to probe down to the molecular level of fibril chiral organization.⁸

Recently it was reported that VCD shows an enhanced sensitivity to amyloid fibril formation and development as demonstrated for lysozyme and insulin.⁹ The observed VCD intensities from fully developed fibrils are one to two orders of magnitude larger than VCD intensities observed from solutions of isolated proteins. It has now been unambiguously demonstrated that this enhanced VCD sensitivity arises from the long-range supramolecular chirality of fibril structure and dynamics at all hierarchical levels.⁸ This sensitivity makes VCD a unique solution-phase, stereo-specific probe of protein fibril chiral structure and correlated fibril morphology.¹⁰ Basic theoretical concepts lead to the conclusion that enhanced VCD spectra as large as those observed from protein fibrils can originate only from supramolecular aggregates that have a long-range chiral organization.¹⁰ For example, insulin and lysozyme fibrils that have an imaged left-handed twist morphology and possess *left-handed helical* proto-filaments, exhibit a distinct VCD spectrum with a sign pattern (+ + - + +), named 'normal VCD'.¹¹ Microscopic examination of protein aggregates formed from other amyloid-associated proteins reveals in some cases a presence of flat, tape-like fibril polymorphs.¹²⁻¹⁵ None of the conventional microscopic techniques, such as cryo-SEM and AFM, have been able to visualize any twist on their surface. Nevertheless, VCD reveals a presence of supramolecular chirality in their supramolecular structure indicating that these tape-like fibrils are composed of *right-handed helical* proto-filaments.⁸ It was found that these tape-like fibrils exhibit a unique VCD spectrum that is close to mirror image with respect to the signs, relative intensities and peak locations, compared to a 'normal' (left-handed) fibril VCD spectrum.

Herein we investigate the supramolecular organization of polyQ fibrils formed from monomers having differing lengths of Q residues. Such fibrils are thought to be important players in the pathology of the expanded CAG-repeat diseases, a family of at least 9 neurodegenerative diseases¹⁶ linked to expanded polyQ sequences in 9 different disease proteins. For example, polyQ aggregates are found in brain autopsies¹⁶, and the repeat-length dependence of spontaneous amyloid formation¹⁷⁻¹⁹ parallels the repeat length

dependences of most of these diseases.¹⁶ Thus, disease risk is minimal for most of these diseases if polyQ repeat length is below about 35, but is high for longer repeat lengths. In contrast to the correlation of aggregation tendencies and rates of disease risk, there has been little evidence for any systematic variation of aggregate morphology with repeat length.

MATERIALS AND METHODS

Preparation of polyglutamine aggregates

All polyglutamine peptides were synthesized at the Small Scale Synthesis facility at the Keck Biotechnology Resource Laboratory of Yale University (<http://keck.med.yale.edu/>) and supplied crude. All peptides were purified and disaggregated as described.²⁰ Aggregation reactions at 37°C in PBS (pH 7.4) were initiated, and monitored by an HPLC-based sedimentation assay. Fibrils of polyglutamine peptides were isolated by centrifuging the final aggregate suspension at 14,000 rpm and re-suspending the pellet with appropriate volume of water to achieve the desired concentration.

Vibrational circular dichroism spectroscopy

VCD and IR spectra were measured at BioTools, Inc, Jupiter, FL using Chiral *IR-2X* Fourier transform VCD (FT-VCD) spectrometer equipped with an MCT detector and the Dual *PEM* option for enhanced VCD baseline stability. For each measurement, ~10 µl of polyQ sample was placed in a *BioCell* (BioTools, Inc.) with CaF₂ windows and a 6-µm pathlength. During measurements the *BioCell* was rotated at a constant velocity about the beam IR axis using SyncRoCell (BioTools, Inc.) to eliminate cell and possible sample birefringence. VCD and IR spectra were acquired for 2–4 hours at 8 cm⁻¹ spectral resolution. Spectral baselines for VCD and IR were determined from measurements of water in the same *BioCell* for the same length of time as sample measurements. All subsequent data processing leading to final spectra was carried out in GRAMS/AI 7.0 (Thermo Galactic, Salem, NH).

Deep ultraviolet resonance Raman (DUVRR) spectroscopy

DUVRR spectra were obtained at the University at Albany using a home-built Raman spectrometer with 199-nm excitation wavelength.²¹ A spinning NMR tube with a magnetic stirrer inside was used for sampling. All reported Raman spectra are an average of at least three independent measurements. In hydrogen-deuterium (H/D) exchange experiments, aggregated polyQ samples were centrifuged at 14 000 rpm for 30 min. The precipitate was separated from the supernatant and washed with D₂O. This procedure was repeated several times. The resulting dispersion of polyQ aggregates in D₂O was incubated overnight at 25°C prior to recording DUVRR spectra. GRAMS/AI 7.0 (Thermo Galactic, Salem, NH) was used for spectral data processing.

Electron microscopy

An aliquot of 5 µl from the fibril suspension was placed on freshly glow-discharged carbon-coated 400-mesh-size copper grid and kept for 2 min before the grid was washed with a drop of deionized water. After that, the sample was stained with freshly filtered 5 µl of 1% (w/v) uranyl acetate for 2 s. The excess of sample, washes and stains was gently blotted off with filter paper. Images were obtained using a Tecnai T12 microscope (FEI) operating at 120 kV and 30,000x magnification and equipped with an UltraScan 1000 CCD camera (Gatan) with post-column magnification of x1.4 (EM facility at Structural Biology Department).

RESULTS AND DISCUSSION

We utilized VCD to investigate the supramolecular chiral organization of polyQ fibrils formed from monomers with Q 30, and Q 35. We also employed deep UV resonance

Raman (DUVRR) spectroscopy coupled with hydrogen-deuterium exchange (H/D) to probe their secondary structure organization and evaluate the solvent accessibility of their β -sheet cores. We found that polyQ monomers of different repeat length not only aggregate at different rates¹⁸ but also form amyloid-like structures with different morphologies as revealed by vibrational spectroscopy. VCD and IR of mature polyQ fibrils in Figure 1 were measured using a Chiral *IR-2X* VCD spectrometer equipped with a Dual *PEM* accessory (BioTools, Inc.).

It was previously shown that IR spectra of polyQ aggregates exhibit typical vibrational modes of Q amino-acid residues (C=O at 1657 cm^{-1} and NH_2 at 1608 cm^{-1}), as well as vibrational modes that originate from the amide chromophores (Amide I at 1626 cm^{-1} and Amide II at 1533 cm^{-1}).^{22–25} While it cannot be ruled out that 1657 cm^{-1} band also contains amide I contributions from other minor amounts of secondary structure, such as alpha-helix or polyproline II, the predominant contribution as been previously established to be side-chain Q C=O stretching. Further, all models of the structure of polyQ fibril aggregates consist of beta-sheet secondary structure. In our analysis here (Figure 1), polyQ aggregates from monomers with different Q repeat lengths showed very similar IR spectra, indicating high similarities in their secondary structure. All samples revealed a sharp Amide I at 1626 cm^{-1} indicating the predominance of β -sheet in their structure.

The VCD spectra of these polyQ aggregates exhibit peaks at six closely correlated frequencies with the sign pattern (- + + + -). Fibrils of Q18, Q25 and Q26 possess nearly the same VCD intensities when normalized by IR with $\Delta A/A$ (g-factor) in the range $\pm 2 \times 10^{-4}$. The magnitude of the VCD intensity is similar to that of the previously observed tape-like insulin fibrils with ‘reversed VCD’. We also found that the intensity of a negative band at 1668 cm^{-1} progressively increases (Figure S1) with the increase of the number of Q residues (Q18 < Q25 < Q26). In contrast, fibrils of Q41 exhibit approximately an order of magnitude greater VCD intensity for all bands compared to the Q18 to Q26 fibrils (Fig. 1a). In particular, dramatic enhancement of VCD band intensity at 1622 cm^{-1} in the spectrum of Q41 fibrils (1626 cm^{-1} in the corresponding IR band) implies the presence of a longer-distance chiral organization of the amide chromophore in the β -sheet structure, not present for Q18 to Q26 fibrils. Moreover, VCD also exhibits a corresponding level of enhancement of the Q side-chain VCD bands at 1668, 1653 and 1606 cm^{-1} . Thus one can deduce that these side-chain groups, along with the main-chain amide groups, are involved in an additional degree of long-range helical chiral organization. In fact it was previously shown that most likely the structure of polyQ fibrils is stabilized by hydrogen bonding by amide units in the polypeptide chain and by the Q side chains.^{24,26} Therefore, polyQ fibrils should be considered as a special class of supramolecular amyloid-fibril polymorphs. Previously we have demonstrated the existence of two classes of amyloid supramolecular polymorphs (left- and right-twisted proto-filaments described above). In those cases, selective formation of either chiral polymorph can be controlled by small variations of the pH during the protein fibrillation. Based on these VCD results, the Q 30 fibrils can be considered as ‘simple chiral’ fibrils with normal enhanced VCD associated with supramolecular chiral structure, while the larger VCD enhancement of Q 35 fibrils should be considered as aggregates with more ‘extensive chiral’ supramolecular organization. Interestingly, this occurs in the absence of any obvious differences in morphology in electron micrographs as shown in Supporting Information (Figure S2), in parallel to the previously discussed inability of AFM and EM to show differences between fibrils that exhibit these VCD differences.

To investigate more closely the dependence of intensity on repeat length shown in Figure 1a), we examined aggregates grown from polyQ peptides Q30, Q35 and Q40. We found that aggregates formed from Q35 monomer exhibited approximately ten times greater VCD intensity compared to Q30 fibrils, yielding a spectrum with an intensity matching that of

Q40 fibrils (Figure S3) as well as Q41 fibrils. In contrast, aggregates formed from Q30 monomer exhibit a VCD spectrum with intensity of all bands similar to those of Q18, Q25 and Q26 fibrils. Despite these differences, the signs and *relative* intensities of all VCD bands for Q 30 and Q 35 fibrils remain the same. Thus, there is only *one* VCD spectrum but it is manifested in two distinct sizes, large (relative to typical isolated protein VCD) for the Q 30 aggregates and very large, an order of magnitude larger, for Q 35 aggregates. These two classes of VCD spectra correspond to two distinct levels of supramolecular chirality. Based on these results, we can conclude that the threshold between these two levels of supramolecular chirality fibrils lies in the region of Q30 to Q35 repeats in the fibril monomer. Ongoing studies in our laboratories should reveal further details about the dramatic repeat length dependent transition between these two ranges of VCD spectral intensities and the corresponding two levels of PolyQ supramolecular chirality.

To gain further insight regarding the relation between polyQ structure and Q repeat length, we utilized deep UV Resonance Raman (DUVRR) spectroscopy coupled with hydrogen deuterium (H/D) exchange to probe the structural organization of polyQ fibril polymorphs. DUVRR spectra of all polyQ aggregates studied (Figure 2a) show amide I^b at $\sim 1660\text{ cm}^{-1}$, amide II^b at $\sim 1550\text{ cm}^{-1}$, C_α-H^b bending at $\sim 1400\text{ cm}^{-1}$, and amide III^b between 1180 and 1330 cm^{-1} .²⁷ As previously reported, the amide I^b band overlaps with the Q side chain amide I^s band; the C_α-H^b band overlaps with the side chain amide III^s+CH₂ peak.²⁷ The high similarity of DUVRR spectra of all polyQ fibrils studied suggests that Q18, Q26 and Q41 fibrils have the same basic secondary structure. Thus, our DUVRR data are highly consistent with the FTIR data discussed above.

At the same time, we found substantial differences in the spectra of Q26 and Q41 fibrils that were exposed to D₂O (Figure 2b). The intensity of both amide II' bands after exchange is substantially higher in the spectrum of Q41 fibrils. This observation suggests that H/D exchange is taking place more extensively in Q41 fibrils than in Q26 fibrils. In spite of the higher stability of Q41 fibrils, the core of Q41 fibrils is thus less protected than the core of Q26 fibrils. A possible explanation of this unexpected observations is that filaments of Q41 fibrils might have a higher degree of helical twist, away from planarity, in their β-sheet core structure compared to that of Q26, thereby weakening the β-sheet hydrogen bonds and allowing greater rates of hydrogen-deuterium exchange. Such an increase in helical twist angle, on the order of a few degrees or less per Q residue, over a large supramolecular structure could be significant in terms of VCD intensity *enhancement* without noticeably changing the local secondary structure that controls the VCD sign pattern and relative intensities. In addition, the complete spectral signature, including intensity scale, of the IR and DUVRR bands would not change since these spectroscopies are not sensitive to long-range supramolecular chiral structure. By postulating an increase in helical twist angle, albeit small without secondary structure change, we are suggesting a structure change that could simultaneously explain the jump in VCD intensity for large Q repeats as well as a subtle change in polyQ structure that gives increased solvent access and with it increased H/D exchange rates.

Due to the similarity of dimensions of the PolyQ fibrils considered here, and amyloid fibrils in general, one might be concerned that the effects observed arise from spurious effects associated with fibril morphology. After having measured scores of PolyQ samples with different numbers of Q-repeats and differing EM morphologies, as shown in Fig. S2, we always observe, as reported here, the same relative VCD pattern. If spurious signals were responsible, or even present above the noise level, for our PolyQ VCD measurements, then the high degree of reproducibility and conservation of relative VCD intensities over many different size variations and morphologies of PolyQ fibrils could not be obtained. Further, there is no evidence from the morphologies of PolQ fibrils for a sudden large increase in

PolyQ VCD intensity. In particular there are no significant changes in the morphological sizes of Q18, Q25, Q26, and Q41 fibrils. Therefore we conclude that spurious effects due to the dimensions of PolyQ fibrils are not present in our VCD spectra.

In addition, our experience with many other fibrils systems, for example lysozyme and insulin, is that the spectra patterns are highly reproducible despite many other variations. In particular, the same frequency and sign pattern for both insulin and lysozyme (VCD spectrum with peaks at 1554, 1593, 1627, 1647, 1670 cm^{-1} , which have a sign pattern (+ + - + +))⁹ is observed despite differences in fibril morphology. In addition, the sense of supramolecular chirality can be controlled by small changes in pH incubation resulting in enhanced VCD with a complete sign reversal of all major fibrils bands (VCD peaks at 1554, 1593, 1627, 1647, 1670 cm^{-1} , which have a sign pattern (+ + - + +)).^{9,28} It also can be mentioned that the VCD spectra of peptide fibrils has been simulated using an oscillator chain model by Measey and Schweitzer-Stenner and was found to be mainly dependent on intrasheet and intersheet vibrational coupling between stacked β -sheets with a small but important backbone twist along the beta-sheet fibril axes.²⁹ Therefore a possibility presence of any spurious VCD signals from the studied polyQ samples can be completely excluded.

It is interesting to contrast these results with other repeat length dependencies of simple polyQ peptides. At the monomer level, there is no evidence in the electronic CD for conformational differences between different repeat length polyQ sequences.³⁰⁻³² There is, however, an enormous increase in aggregation rate with increasing repeat length¹⁸, and polyQ amyloid stability also increases as repeat length increases.¹⁸ The rate effect is linked in part to a decrease in the critical nucleus size for amyloid initiation, from a value of 4 for sequences of Q23 and lower, to a value of 1 for sequences of Q26 and higher.^{20,30} In a cell model for expanded polyQ disease, in which cells die after taking up amyloid fibrils grown in vitro, Q20 amyloid is just as toxic as Q42 amyloid.³³ Likewise, X-ray diffraction showed no gross changes in the cross- β amyloid signature of polyQ aggregates with respect to repeat length, but there was a suggestion that the β -sheets within the amyloid structures from longer polyQ repeats may be wider than from shorter peptides.³⁴

Finally, we note that there is a high degree of similarity of the VCD sign pattern of the polyQ samples reported here and the corresponding VCD sign pattern for a cyclic β -turn-capped left-handed anti-parallel synthetic β -helix peptide consisting of primarily of 18 alternating L- and D-leucine residues.³⁵ While it is premature to conclude anything at this stage regarding the chiral structure of the polyQ fibrils reported here, one possibility that could be considered is that the basic Q-aggregate structural element is a left-twisted anti-parallel structure formed by a β -turn fold. The relation between the core polyQ chiral structures and their VCD spectra will be pursued by planned VCD measurements of additional polyQ fibrils and quantum mechanical VCD calculations of candidate polyQ fibril structures.

CONCLUSIONS

The study of polyQ aggregates using VCD substantially extends our understanding of their supramolecular organization. Despite being microscopically observed as flat un-twisted tapes, these polyQ aggregates exhibit a high order of supramolecular chiral organization that is maintained by both amide chromophore and Q side chains. Both Q 30 and Q 35 fibrils share the same secondary structure; however, they have substantial differences in the details of β -sheet structure, which makes Q 35 fibrils more susceptible to H/D exchange. Both Q 30 and Q 35 fibrils exhibit distinct and specific chiral organization of their secondary structure, which differs substantially from the supramolecular organization of all of previously reported amyloid fibrils.^{8,9}

Finally, Q 35 fibrils exhibit a dramatic enhancement of the VCD intensity without any change of sign or relative intensity of its VCD bands relative to the already enhanced VCD of Q 30 fibrils. This indicates two new, as yet undetermined, levels of supramolecular chirality, one for the Q 30 fibrils and a second for Q 35 fibrils that simply amplifies the VCD without changing the stereo-structural features that determine the VCD of the Q 30 fibrils. One possibility alluded to above is the observed increase in spatial cross-section of the fibril, becoming wider and thicker, without any change in the basic local fibril structure but with some substantial change in the degree of long-range chiral order or the degree of twist of the PolyQ proto-filaments. It seems possible, but remains to be seen, whether the structural differences between amyloid fibrils of Q 35 and Q 30 peptides that are revealed here by VCD and DUVRR spectroscopies are associated with the observed differences in polyQ stability, aggregation rates, as well as toxicity and pathogenicity, of normal length and expanded polyQ sequences.

Supplementary Material

Refer to Web version on PubMed Central for supplementary material.

Acknowledgments

We thank to Ravindra Kodali and Elizabeth Landrum for help with EM images, and Songming Chen for preparation of the fibrils described in the Supporting Information. We also thank Rosina Lombardi for measurement of the VCD spectra in the Supporting Information. This work was supported by grants from the National Institutes of Health, NIH R01 AG019322 (KK and RW) and AG033719 (IL), and grants from the National Science Foundation, SBIR Phase II, IIP-0945484 (RD and LN) and CHE-1152752 (IL).

ABBREVIATIONS

PolyQ	polyglutamine
VCD	vibrational circular dichroism
DUVRR	deep UV resonance Raman
IR	infrared
AFM	atomic force microscopy
EM	electron microscopy
H/D	hydrogen-deuterium

References

1. Chiti F, Dobson CM. Protein misfolding, functional amyloid, and human disease. *Annu Rev Biochem.* 2006; 75:333–66. [PubMed: 16756495]
2. Buxbaum JN, Linke RP. A molecular history of the amyloidoses. *J Mol Biol.* 2012; 421:142–59. [PubMed: 22321796]
3. Goldsbury CS, Cooper GJ, Goldie KN, Muller SA, Saafi EL, Gruijters WT, Misur MP, Engel A, Aebi U, Kistler J. Polymorphic fibrillar assembly of human amylin. *J Struct Biol.* 1997; 119:17–27. [PubMed: 9216085]
4. Rubin N, Perugia E, Goldschmidt M, Fridkin M, Addadi L. Chirality of amyloid suprastructures. *J Am Chem Soc.* 2008; 130:4602–4603. [PubMed: 18338897]
5. Rubin N, Perugia E, Wolf SG, Klein E, Fridkin M, Addadi L. Relation between serum amyloid A truncated peptides and their suprastructure chirality. *J Am Chem Soc.* 2010; 132:4242–4248. [PubMed: 20218685]

6. Kodali R, Wetzel R. Polymorphism in the intermediates and products of amyloid assembly. *Curr Opin Struct Biol.* 2007; 17:48–57. [PubMed: 17251001]
7. Dzwolak W. Vortex-induced chiral bifurcation in aggregating insulin. *Chirality.* 2010; 22(Suppl 1):E154–160. [PubMed: 20845432]
8. Kurouski D, Dukor R, Lu X, Nafie LA, Lednev IK. Normal and Reversed VCD Supramolecular Chirality of Insulin Fibrils. *Biophys J.* 2012; 103:522–531. [PubMed: 22947868]
9. Ma S, Cao X, Mak M, Sadik A, Walkner C, Freedman TB, Lednev IK, Dukor RK, Nafie LA. Vibrational circular dichroism shows unusual sensitivity to protein fibril formation and development in solution. *J Am Chem Soc.* 2007; 129:12364–12365. [PubMed: 17894496]
10. Nafie, LA. *Vibrational Optical Activity: Principles and Applications.* Wiley; Chichester: 2011.
11. Kurouski D, Lombardi RA, Dukor RK, Lednev IK, Nafie LA. Direct observation and pH control of reversed supramolecular chirality in insulin fibrils by vibrational circular dichroism. *Chem Commun.* 2010; 46:7154–7156.
12. Anderson M, Bocharova OV, Makarava N, Breydo L, Salnikov VV, Baskakov IV. Polymorphism and ultrastructural organization of prion protein amyloid fibrils: an insight from high resolution atomic force microscopy. *J Mol Biol.* 2006; 358:580–596. [PubMed: 16519898]
13. Bauer HH, Aebi U, Haner M, Hermann R, Muller M, Merkle HP. Architecture and polymorphism of fibrillar supramolecular assemblies produced by in vitro aggregation of human calcitonin. *J Struct Biol.* 1995; 115:1–15. [PubMed: 7577226]
14. Cardoso I, Goldsbury CS, Muller SA, Olivieri V, Wirtz S, Damas AM, Aebi U, Saraiva MJ. Transthyretin fibrillogenesis entails the assembly of monomers: a molecular model for in vitro assembled transthyretin amyloid-like fibrils. *J Mol Biol.* 2002; 317:683–695. [PubMed: 11955017]
15. Jimenez JL, Nettleton EJ, Bouchard M, Robinson CV, Dobson CM, Saibil HR. The protofilament structure of insulin amyloid fibrils. *Proc Natl Acad Sci U S A.* 2002; 99:9196–9201. [PubMed: 12093917]
16. Bates, GP.; Benn, C. The polyglutamine diseases. In: Bates, GP.; Harper, PS.; Jones, L., editors. *Huntington's Disease.* Oxford University Press; Oxford: 2002. p. 429-472.
17. Scherzinger E, Sittler A, Schweiger K, Heiser V, Lurz R, Hasenbank R, Bates GP, Lehrach H, Wanker EE. Self-assembly of polyglutamine-containing huntingtin fragments into amyloid-like fibrils: implications for Huntington's disease pathology. *Proc Natl Acad Sci U S A.* 1999; 96:4604–4609. [PubMed: 10200309]
18. Chen S, Berthelie V, Yang W, Wetzel R. Polyglutamine aggregation behavior in vitro supports a recruitment mechanism of cytotoxicity. *J Mol Biol.* 2001; 311:173–182. [PubMed: 11469866]
19. Morley JF, Brignull HR, Weyers JJ, Morimoto RI. The threshold for polyglutamine-expansion protein aggregation and cellular toxicity is dynamic and influenced by aging in *Caenorhabditis elegans*. *Proc Natl Acad Sci U S A.* 2002; 99:10417–10422. [PubMed: 12122205]
20. Kar K, Jayaraman M, Sahoo B, Kodali R. Critical nucleus size for disease-related polyglutamine aggregation is repeat-length dependent. *Nat Struct Mol Biol.* 2011; 18:328–336. [PubMed: 21317897]
21. Lednev IK, Ermolenkov VV, He W, Xu M. Deep-UV Raman spectrometer tunable between 193 and 205 nm for structural characterization of proteins. *Anal Bioanal Chem.* 2005; 381:431–437. [PubMed: 15625596]
22. Mishra R, Jayaraman M, Roland BP, Landrum E, Fullam T, Kodali R, Thakur AK, Arduini I, Wetzel R. Inhibiting the nucleation of amyloid structure in a huntingtin fragment by targeting alpha-helix-rich oligomeric intermediates. *J Mol Biol.* 2011; 415:900–917. [PubMed: 22178478]
23. Sivanandam VN, Jayaraman M, Hoop CL, Kodali R, Wetzel R, van der Wel PC. The aggregation-enhancing huntingtin N-terminus is helical in amyloid fibrils. *J Am Chem Soc.* 2011; 133:4558–4566. [PubMed: 21381744]
24. Sikorski P, Atkins E. New model for crystalline polyglutamine assemblies and their connection with amyloid fibrils. *Biomacromolecules.* 2005; 6:425–432. [PubMed: 15638548]
25. Jayaraman M, Kodali R, Sahoo B, Thakur AK, Mayasundari A, Mishra R, Peterson CB, Wetzel R. Slow amyloid nucleation via alpha-helix-rich oligomeric intermediates in short polyglutamine-containing huntingtin fragments. *J Mol Biol.* 2012; 415:881–899. [PubMed: 22178474]

26. Perutz MF, Pope BJ, Owen D, Wanker EE, Scherzinger E. Aggregation of proteins with expanded glutamine and alanine repeats of the glutamine-rich and asparagine-rich domains of Sup35 and of the amyloid beta-peptide of amyloid plaques. *Proc Natl Acad Sci U S A*. 2002; 99:5596–5600. [PubMed: 11960015]
27. Xiong K, Punihaole D, Asher SA. UV Resonance Raman Spectroscopy Monitors Polyglutamine Backbone and Side Chain Hydrogen Bonding and Fibrillization. *Biochemistry*. 2012; 51:5822–5830. [PubMed: 22746095]
28. Kurouski D, Dukor RK, Lu X, Nafie LA, Lednev IK. Spontaneous inter-conversion of insulin fibril chirality. *Chem Commun*. 2012; 48:2837–2839.
29. Measey T, Schweitzer-Stenner R. Vibrational circular dichroism as a probe of fibrillogenesis: the origin of the anomalous intensity enhancement of amyloid-like fibrils. *J Am Chem Soc*. 2010; 133:1066–1067. [PubMed: 21186804]
30. Chen S, Ferrone FA, Wetzel R. Huntington's disease age-of-onset linked to polyglutamine aggregation nucleation. *Proc Natl Acad Sci U S A*. 2002; 99:11884–11889. [PubMed: 12186976]
31. Masino L, Kelly G, Leonard K, Trottier Y, Pastore A. Solution structure of polyglutamine tracts in GST-polyglutamine fusion proteins. *FEBS Lett*. 2002; 513:267–272. [PubMed: 11904162]
32. Chen S, Berthelie V, Hamilton JB, O'Nuallain B, Wetzel R. Amyloid-like features of polyglutamine aggregates and their assembly kinetics. *Biochemistry*. 2002; 41:7391–7399. [PubMed: 12044172]
33. Yang W, Dunlap JR, Andrews RB, Wetzel R. Aggregated polyglutamine peptides delivered to nuclei are toxic to mammalian cells. *Hum Mol Genet*. 2002; 11:2905–2917. [PubMed: 12393802]
34. Sharma D, Shinchuk LM, Inouye H, Wetzel R, Kirschner DA. Polyglutamine homopolymers having 8–45 residues form slablike beta-crystallite assemblies. *Proteins*. 2005; 61:398–411. [PubMed: 16114051]
35. Kulp JL 3rd, Owrutsky JC, Petrovykh DY, Fears KP, Lombardi R, Nafie LA, Clark TD. Vibrational circular-dichroism spectroscopy of homologous cyclic peptides designed to fold into beta helices of opposite chirality. *Biointerphases*. 2011; 6:1–7. [PubMed: 21428689]

HIGHLIGHTS

PolyQ fibril aggregates exhibit enhanced VCD and supramolecular chiral organization that differ from all previously observed amyloid fibrils.

Q 35 aggregates show a further enhanced level of supramolecular chiral organization compared to Q 30 aggregates.

Q 35 and Q 30 fibril aggregates exhibit the same secondary structure and VCD intensity pattern.

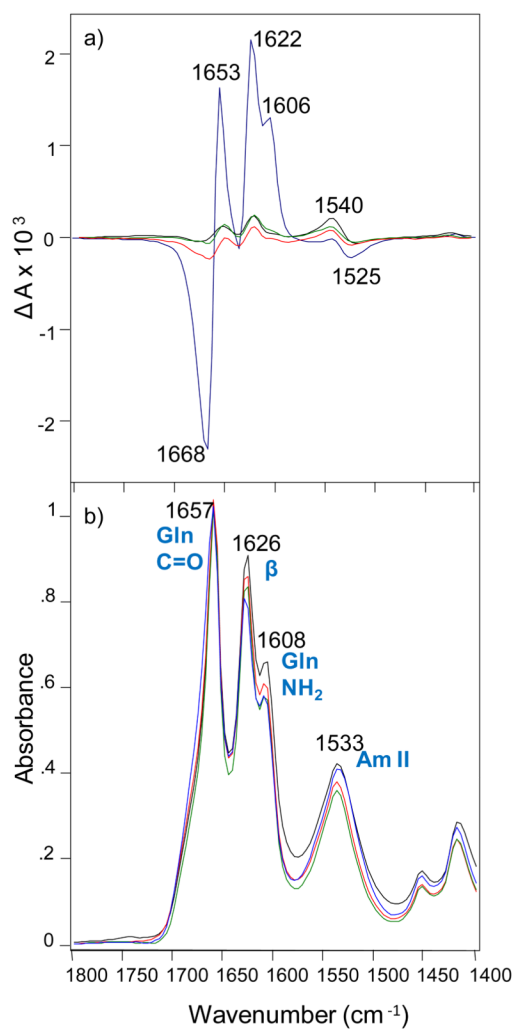


Figure 1. VCD (a) and IR (b) spectra of Q 41 aggregates (blue), Q 26 aggregates (red), Q 25 aggregates (green) and Q 18 aggregates (black).

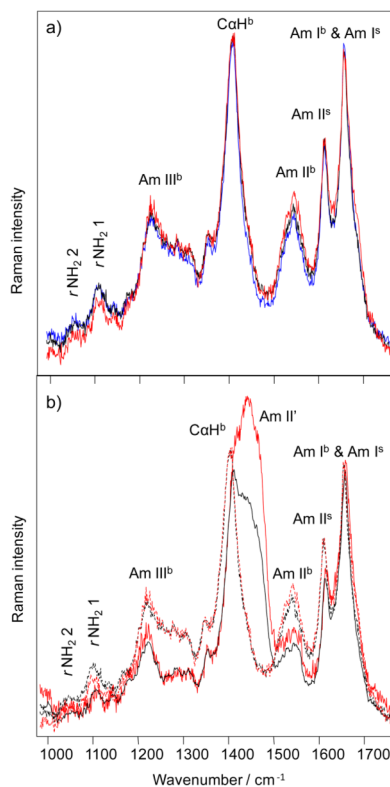


Figure 2. DUVRR spectra of polyQ aggregates in water (a): Q18 (blue), Q26 (black) and Q41 (red) aggregates. H/D exchange spectra (b) of Q41 aggregates (red) and Q 26 aggregates (black). Their corresponding spectra in water are shown by dashed lines. Subscripts ^b and ^s stand for backbone and side chain, respectively.²⁷